Irrig Sci (2009) 27:223–229
DOI 10.1007/s00271-008-0137-9

ORIGINAL PAPER

Estimating in situ soil–water retention and field water capacity in two contrasting soil textures

J. D. Jabro · R. G. Evans · Y. Kim · W. M. Iversen

Received: 6 June 2008 / Accepted: 9 October 2008 / Published online: 1 November 2008

Abstract A priori knowledge of the in situ soil field water capacity (FWC) and the soil-water retention curve for soils is important for the effective irrigation management and scheduling of many crops. The primary objective of this study was to estimate the in situ FWC using the soil-water retention curve developed from volumetric water content (θ), and water potential (ψ) data collected in the field by means of soil moisture sensors in two contrasting-textured soils. The two study soils were Lihen sandy loam and Savage clay loam. Six metal frames 117 cm × 117 cm × 30 cm high were inserted into the soil to a depth of 5–10 cm at approximately 40 m intervals on a 200 m transect. Two Time Domain Reflectrometry (TDR) sensors were installed in the center of the frame and two Watermark (WM) sensors were installed in the SW corner at 15 and 30 cm depths to continuously monitor soil θ and ψ, respectively. A neutron probe (NP) access tube was installed in the NE corner of each frame to measure soil θ used for TDR calibration. The upper 50–60 cm of soil inside each frame was saturated with intermittent application of approximately 18–20 cm of water. Frames were then covered with plastic tarps. The Campbell and Gardner equations best fit the soil–water retention curves for sandy loam and clay loam soils, respectively. Based on the relationship between soil ψ and elapsed time following cessation of infiltration, we calculated that the field capacity time (t_{FWC}) were reached at approximately 50 and 450 h, respectively, for sandy loam and clay loam soils. Soil-water retention curves showed that θ values at FWC (θ_{FWC}) were approximately 0.228 and 0.344 $m^3\ m^{-3}$, respectively, for sandy loam and clay loam soils. The estimated θ_{FWC} values were within the range of the measured θ_{FWC} values from the NP and gravimetric methods. The TDR and WM sensors provided accurate in situ soil–water retention data from simultaneous soil θ and ψ measurements that can be used in soil-water processes, irrigation scheduling, modeling and chemical transport.

List of symbols

ψ	soil matric potential
ψ_e	air-entry water potential
θ	volumetric soil–water content
θ_s	saturated water content
a, b	empirically constants determined from the soil–water retention curve
θ_r	residual water content
t	elapsed time following cessation of infiltration
a, t_0 and b	model fitting parameters
FWC	field water capacity
θ_{FWC}	soil–water content at field water capacity
t_{FWC}	field water capacity time

Introduction

In most soils, optimal irrigation management practices for many crops require measurement or estimation of soil–water retention data in the field or laboratory to assess both the amount and timing of irrigation. A water retention

Communicated by S. Ortega-Farias.

J. D. Jabro (✉) · R. G. Evans · Y. Kim · W. M. Iversen
Northern Plains Agricultural Research Laboratory, USDA-ARS, 1500 N. Central Avenue, Sidney, MT 59270, USA
e-mail: jay.jabro@ars.usda.gov

curve, also called as the soil moisture characteristic curve, describes the "functional relationship between the soil–water content θ, and soil matric potential ψ in unsaturated soils that is characteristic for different types of soil" (Hanks and Ashcroft 1980; Taylor and Ashcroft 1972). The curve, a basic soil property is affected by soil physical and chemical characteristics; e.g., soil texture, structure, amount and degree of aggregates, amount of colloids, type of clay mineral, and amount of soluble salts (Hillel 1971; Taylor and Ashcroft 1972; Kirkham 2005).

A priori knowledge of the soil–water retention curve is also essential in modeling of water flow and chemical transport in soils, in estimating the available water holding capacity and in simulating of soil–water behavior and relations in unsaturated soils (Pachepsky et al. 2001; Prunty and Casey 2002). The curve is used to study irrigation, drainage, aggregate stability, soil infiltration, hydraulic conductivity, the available water holding capacity of plants (the difference between soil field water capacity and permanent wilting point), and chemical transport (Hillel 1971; Taylor and Ashcroft 1972; Hanks and Ashcroft 1980).

The in situ field water capacity (FWC) "is the content of water on a mass or volume basis, remaining in a soil 2 or 3 days after the soil having been wetted with water and after free drainage is negligible" (http://www.soils.org/sssagloss, verified 23 April 2008). It is the upper limit of water content that a soil can hold against gravitational force when all soil macropores have been drained and replaced with air (Hillel 1980; Lal and Shukla 2004). After soil infiltration ceases and equilibrium is reached, water within the wetted portion of the soil profile drains to deeper depths under the influence of soil potential gradients. The downward movement of water in the soil profile is relatively fast initially, decreases rapidly with time (Hillel 1971; Taylor and Ashcroft 1972; Hillel 1980).

According to Kirkham (2005) and others, FWC is neither a soil constant nor a soil property but is considered as a vague yet qualitatively useful estimate in many soil–water–plant relations applications. soil–water content at the FWC level is considered optimal for many growing crops in most soils (Warrick 2002).

The FWC is perhaps more applicable to sandy soils than to clay soils, because sandy-textured soils hold less water and drain relatively faster than clayey-textured soils. In sandy soils, most of the pores drain shortly after a rainfall or irrigation and the capillary conductivity in these soils becomes negligibly small at high soil–water matric potentials compared to clayey soils (Gardner 1960; Gardner et al. 1970; Hillel 1971; Smith and Warrick 2007).

Many attempts have been made to relate FWC to soil–water retention at a particular soil matric potential, often to the −33 kPa (−1/3 bar); thus, the physical definition of field capacity by many agronomists, soil scientists and agricultural engineers is considered the bulk water content retained in the soil at −33 kPa (−1/3 bar) of soil matric potential or suction (tension), ψ (Hillel 1971; Taylor and Ashcroft 1972; Hanks and Ashcroft 1980; Jury et al. 1991; Kirkham 2005). However, FWC is not a unique value but is expressed as a range of values of soil–water content (Kirkham 2005). It is influenced by many factors such as initial soil–water content, soil texture and structure, type of clay, presence of or amount of organic matter, presence of water table, presence of impeding layer and evapotranspiration (Kirkham 2005). Nevertheless, the term FWC is often misunderstood (Warrick 2002) and little research has been done on estimating FWC and developing in situ soil–water retention curves using newly developed soil moisture sensors.

These sensors including Watermark (WM) and Time Domain Reflectrometry (TDR) can be datalogged for continuous measurements of soil θ and ψ at various depths in the soil profile (Leib et al. 2003). These continuously monitoring sensors have recently been used in soil–water content measurements for a variety of agricultural and environmental applications including irrigation management and scheduling (Dane and Hopmans 2002). Nevertheless, the relationship developed between soil ψ measured by WM resistance blocks and soil θ measured by the TDR must be determined before these sensors can be used effectively in irrigation scheduling and management (Morgan et al. 2001).

The objective of this work was to estimate in situ FWC from a soil–water retention curve developed with soil ψ and θ data collected in the field using WM and TDR sensors, respectively, in two contrasting textured soils.

Materials and methods

Experimental sites and soils

Soil–water content θ, and soil matric potentials ψ were measured at two sites of different soil texture, one in North Dakota and the other in Montana. The North Dakota site (Nesson) is located at the Nesson Valley Research farm, approximately 37 km east of Williston, ND, at latitude 48.1640°N and longitude 103.0986°W. The soil is mapped as Lihen sandy loam (sandy, mixed, frigid Entic Haplustoll) and consists of very deep, somewhat excessively or well drained, nearly level soil that formed in sandy alluvium, glacio-fluvial, and eolian deposits. The Montana site at the Montana State University Eastern Agricultural Research Center (EARC) is located approximately 2 km north of Sidney, MT, at latitude 47.7255°N and longitude 104.1514°W. The soil at the EARC site is classified as Savage clay loam (fine, smectitic, frigid Vertic Argiustolls)

Table 1 Selected soil physical properties

Soil[a]	Depth (cm)	Sand (g kg^{-1})	Silt (g kg^{-1})	Clay (g kg^{-1})	Bulk density (Mg m^{-3})
Sandy loam	0–15	660	170	170	1.56
	15–30	670	150	180	1.51
Clay loam	0–15	210	410	380	1.43
	15–30	200	430	370	1.39

[a] Each value was replicated 6 times

and consists of deep, drained, nearly level soils formed in alluvium parent material. Selected soil physical properties for both soils are given in Table 1.

Field procedures

The experiments comprising in situ field water capacity (FWC) and the soil–water retention curves were conducted in fall 2006 and spring 2007 for the Nesson and EARC sites, respectively. Using a tractor front loader, at each site we inserted 6 metal frames 117 cm × 117 cm, 30 cm high into the soil to a depth of 5–10 cm to prevent lateral water movement for each site (Fig. 1). The frames were spaced at approximately 40 m intervals on a 200 m transect to account for soil variability across the field. Two TDR sensors (CS625, Campbell Scientific Inc., Logan, UT) were installed in the center of the frame and two WM sensors (Irrometer company, Riverside, CA) were installed in the southwest (SW) corner at 15 and 30 cm depths at the EARC site to continuously monitor changes in volumetric soil–water content and soil–water matric potential, respectively (Fig. 1). At the Nesson site, the TDR sensors were installed vertically in the center of the frame.

Fig. 1 Schematic of the experimental setup. The sensors are installed in the soil inside the metal frame

Sensor installation processes and operational procedures were carried out according to the manufacturer's recommendations and instructions (http://www.campbellsci.com; http://www.irrometer.com). Data from TDR and WM sensors at both sites were recorded hourly.

A NP access tube was installed in the NE corner of each frame to measure the soil–water content used to calibrate TDR measurements (Fig. 1). The NP readings were taken every 6 h in sandy loam and daily in clay loam soil. The soil profile in the framed area was thoroughly saturated to a depth of 50–60 cm depth by intermittent application of approximately 18–20 cm of water. The remaining ponded water on the soil surface was allowed to infiltrate. After all water had been infiltrated, the frames were covered with plastic tarps, secured to the frames with duct tape to avoid any evaporation from the soil. Measurements of soil ψ and θ were monitored continuously at two depths using WM and TDR sensors, respectively, for approximately 50 h in sandy loam and 19 days in clay loam soil under internal drainage (redistribution). Neutron probe measurements were also taken at two depths in each framed area during the redistribution process and at the end of the experiment.

The time at which soil–water redistribution or internal drainage becomes nearly negligible as the change of soil ψ over elapsed time approaches zero is the field water capacity time t_{FWC}.

At the end of the experiment, nine soil cores were taken at the 0–10, 10–20 and 20–30 cm depths at 3 cores per depth around the center of each framed area to determine soil gravimetric water content.

Sensor descriptions

A brief description of each sensor used in this study is provided and indicates the sensor's measurement principle, installation process and manufacturer.

Neutron probe (NP)

The NP device consists of a source of fast neutrons and a detector housed in a probe that is lowered into an access tube installed in the soil. Fast neutrons emitted from the source collide with hydrogen molecules in the soil–water and are slowed down by the collision. The slow neutrons that return to the probe are counted by the detector and this count is linearly related to the volumetric moisture content (Gardner 1986; http://www.cpn-bj.com.cn). A galvanized steel access tube (38.1 mm in diameter) was installed by auguring a hole of the same diameter and inserting the access tube.

Watermark soil moisture sensors (WM)

The WM sensor consists of an electrical resistance block with two electrodes in a gypsum wafer surrounded by a granular matrix material encased in a perforated cylindrical stainless steel case. The electrodes measure the electrical resistance, which is a function of the water content inside the sensors and varies inversely with water content in the soil (http://www.irrometer.com).

The WM sensors were attached to a 1.27 cm PVC pipe that allowed sensors to be pushed into the access hole at desired depths during installation. A PVC cap was used to close the top of the pipe to prevent rain or irrigation water from entering the pipe.

A temperature sensor was installed in the soil above the WM sensors for correction of WM readings; the WM sensor was calibrated for a soil temperature of 21°C. A 2.54-cm soil auger was used to place the WM sensor at two depths with soil slurry to ensure good contact. Soil ψ and temperature readings were continuously recorded using a WM monitor datalogger. The WM sensor measures soil matric potentials in centibars (cbar), equivalent to kilopascal (kPa) over a range of 0 to −200 cbar or kPa (Irrometer Co. of Riverside, CA; http://www.irrometer.com).

Time Domain Reflectrometry (TDR)

The TDR sensor (CS625, Campbell Scientific Inc., Logan, UT; http://www.campbellsci.com) consists of two stainless steel rods connected to a printed circuit board encapsulated in epoxy. A shielded four-conductor cable is connected to the circuit board to supply power, facilitate the probe, and monitor the pulse output. The CS625's square wave output can be connected to a Campbell Scientific CR200 datalogger; its frequency depends on the dielectric permittivity of the media surrounding the stainless steel rods. The dielectric permittivity is affected primarily by the water content of the soil. The CS625 utilizes a CRBasic program using period averaging to measure the probe output period and convert to volumetric water content (http://www.campbellsci.com).

The probe rods were installed horizontally to the soil surface in clay loam soil and vertically in sandy loam soil. The rods were kept as parallel as possible using an insertion pilot tool to maintain the design wave guide geometry.

Results and discussion

The in situ soil–water retention data from simultaneous soil ψ and volumetric θ measurements recorded with the WM and TDR sensors for both sandy loam and clay loam soils are presented in Figs. 2 and 3, respectively. The mean

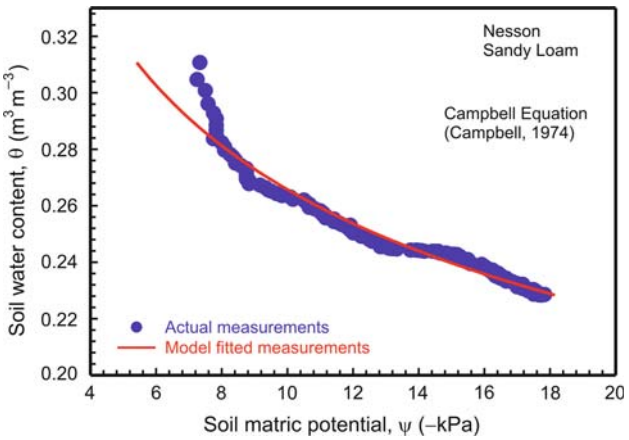

Fig. 2 Soil–water retention curve for sandy loam soil at Nesson location

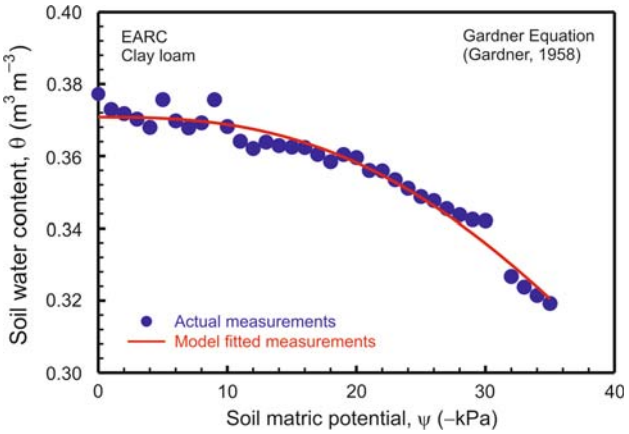

Fig. 3 Soil–water retention curve for clay loam soil at the EARC location

values of soil ψ and volumetric θ at the 0–15 and 15–30 cm depths from all 6 frames were used to develop soil–water retention curves at each location as soils at these 2 layers were nearly homogeneous and uniform in texture and structure properties (Table 1).

A number of curve equations for soil–water characteristics were examined to determine which equation best fit the relationship between soil ψ and volumetric θ data (Leong and Rahardjo 1997). The Campbell (1974) equation (Eq. 1) provides the best fit for the water retention curve with $R^2 = 0.97$ for sandy loam soil (Fig. 2).

$$\psi = \psi_e \left(\frac{\theta}{\theta_s}\right)^{-b} \quad (1)$$

where ψ is the soil matric potential, ψ_e is the air-entry water potential, θ is the volumetric soil–water content, θ_s is the saturated water content, and b is empirically determined from the soil–water retention curve (Campbell 1974).

Table 2 Models' fitting parameters

Equation number	Fitting parameters			
Eqs. 1 and 2 (Campbell 1974)	ψ_e (kPa) = 1.637	θ_s (m^3 m^{-3}) = 0.421	b = 3.934	
Eqs. 3 and 4 (Gardner 1958)	θ_r (m^3 m^{-3}) = $1.86 \times 10^{-10} \approx 0$	θ_s (m^3 m^{-3}) = 0.371	a = 70.1	b = 2.667
Eq. 5	a = 18.71	t_0 (h) = 13.32	b = 12.67	
Eq. 6	a = 57.47	t_0 (h) = 614	b = −0.80	

Equation 1 can also be rearranged and solved in terms of soil volumetric water content as:

$$\theta = \theta_s \left(\frac{\psi}{\psi_e}\right)^{-1/b} \quad (2)$$

Equation 2 converts the soil matric potential directly to soil volumetric water content.

Figure 3 shows an in situ soil–water retention curve for a clay loam soil that is best described using the Gardner equation (Eq. 3) with $R^2 = 0.96$ (Gardner 1958).

$$\theta = \theta_r + \frac{\theta_s - \theta_r}{1 + \left(\frac{\psi}{a}\right)^b} \quad (3)$$

where θ_r is the residual water content, θ_s is the saturated water content, a and b are empirically determined from the soil–water retention curve (Gardner 1958). The preceding equation is more commonly referred to as a logistic four-parameter curve (Seber and Wild 1989). The estimated θ_r for this data set was too small because of the wet soil conditions used in this study (between saturation and FWC) and was therefore set to zero. Equation 3 was then simplified using $\theta_r = 0$ as:

$$\theta = \frac{\theta_s}{1 + \left(\frac{\psi}{a}\right)^b} \quad (4)$$

Equation 4 can be used to estimate θ at any given value of ψ using soil–water retention data. The fitting parameters for Eqs. 1, 2, 3 and 4 are listed in Table 2.

Field water capacity (FWC) estimation

The change of soil ψ over elapsed time following cessation of infiltration for both sandy loam and clay loam soils are plotted in Figs. 4 and 5, respectively. Figure 4 shows a data set of water potential for a sandy loam that is best fit by a 3-parameter sigmoid model ($R^2 = 0.997$) as is given in Eq. 5 (Leong and Rahardjo 1997):

$$\psi = \frac{a}{1 + e^{\frac{-(t-t_0)}{b}}} \quad (5)$$

The data for clay loam soil at the EARC location (Fig. 5) was on the other hand, well described by a

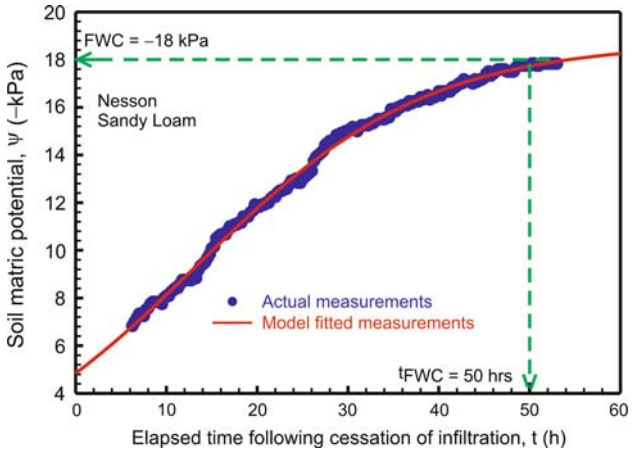

Fig. 4 Soil matric potential as a function of time for sandy loam soil at the Nesson location

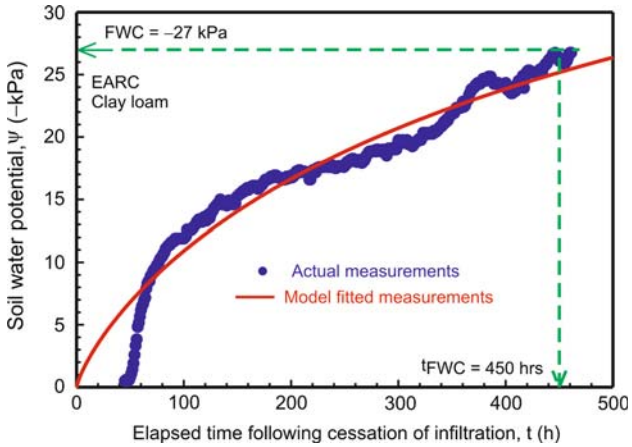

Fig. 5 Soil matric potential as a function of time for clay loam soil at the EARC location

3-parameter sigmoid logistic model ($R^2 = 0.936$) (Leong and Rahardjo 1997) as follows:

$$\psi = \frac{a}{1 + \left(\frac{t}{t_0}\right)^b} \quad (6)$$

where ψ is the soil matric potential, t is the elapsed time following cessation of infiltration, and a, t_0 and b are model fitting parameters. The fitting parameters for Eqs. 5 and 6 are listed in Table 2.

Table 3 Measured and estimated soil–water contents, θ at field water capacity, θ_{FWC}

Location	Soil	Soil–water content at the field water capacity, θ_{FWC} (m^3 m^{-3})		
		Gravimetric method Mean ± 2 SE	Neutron probe	Estimated from the TDR sensor
Nesson	Sandy loam	0.213 ± 0.011	0.222 ± 0.013	0.228
EARC	Clay loam	0.315 ± 0.021	0.351 ± 0.014	0.344

Equations 5 and 6 were fitted to the measured data using a non-linear least squares optimization approach that minimizes the sum of squared deviations between measured and fitted soil–water matric potentials (Seber and Wild 1989; http://www.systat.com; http://www.SAS.com).

Figures 4 and 5 show the rate of water redistribution in the soil profile as the gradients of soil–water potential ($d\psi/dt$) decrease. Thus, soil–water content loss or redistribution from the upper soil profile after cessation of infiltration, rapid at the beginning, becomes gradually slower and slower, and in time this loss in θ becomes very small (Figs. 4, 5), reaching approximately equilibrium conditions (Hillel 1971, 1980).

The time at which the soil internal drainage or redistribution process becomes nearly negligible as the gradient of water content ($d\theta/dt$ or $d\psi/dt$) approaches zero is the time at which field water capacity time, t_{FWC} (Hillel 1971; Romano and Santini 2002). The t_{FWC} for both soils was estimated from the actual data at the plateau at equilibrium using WM sensor data (Figs. 4, 5). Furthermore, the fitted equations (Eqs. 5, 6) produce t_{FWC} values close to those estimated by the sensors at very small values of slope of line or gradient ($d\psi/dt$).

Based on our results, the t_{FWC} for both sandy loam and clay loam soils used in this study were reached at approximately 50 and 450 h following cessation of soil infiltration, respectively (Figs. 4, 5). Ratliff et al. (1983) suggested that negligible internal drainage occurs when soil θ decreases by approximately 0.1–0.2% (Romano and Santini 2002). Using relationships presented in Figs. 4 and 5, the soil ψ values at the field water capacity level, ψ_{FWC}, at t_{FWC} of 50 and 450 h were approximately −18 and −27 kPa for sandy loam and clay loam soils, respectively. Based on soil–water retention curves presented in Figs. 2 and 3, the equivalent θ values at field water capacity, θ_{FWC}, were approximately 0.228 and 0.344 m^3 m^{-3} for sandy loam (Nesson) and clay loam (EARC) soils, respectively. The θ_{FWC} acquired from the gravimetric and NP measurements at the end of the experiment are given in Table 3. Results reported in Table 3 show that the estimated θ_{FWC} values were within the range of the measured θ_{FWC} values from the NP and gravimetric water content methods. These results indicate that WM and TDR sensors are useful for estimating θ_{FWC} and provide accurate in situ soil–water retention data that can be used in agricultural, environmental and modeling applications including irrigation management and scheduling.

Conclusions

The in situ soil–water retention curves from simultaneous soil ψ and volumetric θ measurements obtained from the WM and TDR sensors were developed for both sandy loam and clay loam soils.

The Campbell (1974) and Gardner (1958) equations provided the best fit for the soil–water retention curves with $R^2 = 0.97$ and 0.96 for sandy loam and clay loam soils, respectively.

The changes of soil ψ with time following cessation of infiltration were well described by 3-parameter sigmoid models with $R^2 = 0.997$ and 0.936 for sandy loam and clay loam soils, respectively. Based on these relationships, the t_{FWC} were reached at approximately 50 and 450 h following cessation of infiltration and soil ψ_{FWC} values at these two elapsed times were approximately −18 and −27 kPa for sandy loam and clay loam soils, respectively. Using soil–water retention curves, the corresponding θ_{FWC} values at 50 and 450 h were approximately 0.228 and 0.344 m^3 m^{-3} for sandy loam (Nesson) and clay loam (EARC) soils, respectively.

The estimated θ_{FWC} values were within the range of the measured θ_{FWC} values obtained from the NP probe and gravimetric methods. These results indicated that WM and TDR sensors provided accurate in situ soil–water retention data that can be used in agricultural and environmental applications including irrigation management and scheduling.

Acknowledgments The authors sincerely thank Mr. Dale Spracklin for his help in installing soil moisture sensors, monitoring the experiments and collecting and processing soil samples. The helpful suggestions of the Editor, Dr. Samuel Ortega-Farias and three anonymous reviewers are greatly appreciated.

Appendix

Fitted equations and their derivatives:

$$\psi = \psi_e \left(\frac{\theta}{\theta_s}\right)^{-b}, \quad \text{Campbell (1974)} \tag{1}$$

$$\frac{d\psi}{d\theta} = \psi_e \left(\frac{\theta}{\theta_s}\right)^{-b} \frac{b}{\theta}$$

$$\theta = \theta_s \left(\frac{\psi}{\psi_e}\right)^{-1/b}, \quad \text{Campbell (1974)} \tag{2}$$

$$\frac{d\theta}{d\psi} = -\theta_s \frac{\left(\frac{\psi}{\psi_e}\right)^{-1/b}}{b\theta}$$

$$\theta = \frac{\theta_s}{1 + \left(\frac{\psi}{a}\right)^b}, \quad \text{Gardner (1958)} \tag{4}$$

$$\frac{d\theta}{d\psi} = \frac{-\theta_s \left(\frac{\psi}{a}\right)^b \frac{b}{\psi}}{\left(1 + \left(\frac{\psi}{a}\right)^b\right)^2}$$

$$\psi = \frac{a}{1 + e^{\frac{-(t-t_0)}{b}}}, \text{ 3-parameter sigmoid logistic model} \tag{5}$$

$$\frac{d\psi}{dt} = \frac{a e^{\frac{-(t-t_0)}{b}}}{\left(1 + e^{\frac{-(t-t_0)}{b}}\right)^2 b}$$

$$\psi = \frac{a}{1 + \left(\frac{t}{t_0}\right)^b}, \text{ 3-parameter sigmoid model} \tag{6}$$

$$\frac{d\psi}{dt} = \frac{-a \left(\frac{t}{t_0}\right)^b \frac{b}{t}}{\left(1 + \left(\frac{t}{t_0}\right)^b\right)}$$

References

Campbell GS (1974) A simple method for determining unsaturated conductivity from moisture retention data. Soil Sci 117:311–314

Dane JH, Hopman JW (2002) Water retention and storage. In: Dane JH, Topp GC (eds) Methods of soil analysis: Part 4—Physical methods. SSSA Book Ser. 5. SSSA, Madison

Gardner WR (1958) Some steady state solutions of the unsaturated moisture flow equation with application to evaporation from a water table. Soil Sci 85:228–232

Gardner WR (1960) Dynamic aspects of water availability to plants. Soil Sci 89:63–73

Gardner WH (1986) Water content. In: Klute A (ed) Methods of soil analysis. Part 1. Physical and mineralogical methods, 2nd edn. Agronomy Monogr. 9. ASA and SSSA, Madison, pp 635–662

Gardner WH, Hillel D, Benyamini Y (1970) Post-irrigation movement of soil water. 1: redistribution. Water Resour Res 6:851–861

Hanks RJ, Ashcroft GL (1980) Applied soil physics. Springer, Berlin

Hillel D (1971) Soil and water, physical principles and processes. Academic press, New York

Hillel D (1980) Fundamentals of soil physics. Academic press, New York

Jury W, Gardner WR, Gardner WH (1991) Soil Physics. Wiley, New York

Kirkham MB (2005) Principles of soil and plant water relations. Elsevier, Burlington

Morgan KT, Parsons LR, Wheaton A (2001) Comparison of laboratory- and field derived soil water retention curves for a fine soil using tensiometric, resistance and capacitance methods. Plant Soil 234:153–157

Lal R, Shukla MK (2004) Principles of soil physics. Marcel Dekker, Inc., New York

Leong EC, Rahardjo H (1997) Review of soil–water characteristic curve equations. J Geotech Geoenviron Eng 123:1106–1117

Leib BG, Jabro JD, Matthews GR (2003) Field evaluation and performance comparison of soil moisture sensors. Soil Sci 168:396–408

Pachepsky Y, Rawls W, Gimenez D (2001) Comparison of soil water retention at field and laboratory scales. Soil Sci Soc Am J 65:460–462

Prunty L, Casey FM (2002) Soil water retention curve description using a flexible smooth function. Vadose Zone J 1:179–185

Ratliff LF, Ritchie JT, Cassel DK (1983) Field-measured limits of soil water availability as related to laboratory-measured properties. Soil Sci Soc Am J 47:770–775

Romano N, Santini A (2002) Field water capacity. In: Dane JH, Topp GC (eds) Methods of soil analysis: Part 4—Physical methods. SSSA Book Ser. 5. SSSA, Madison, pp 722–738

Seber G, Wild CJ (1989) Nonlinear regression. Wiley, New York

Smith RE, Warrick AW (2007) Soil water relationships. In: Hoffman GJ, Evans RG, Jensen ME, Martin DL, Elliott RL (eds) Design and operation of farm irrigation systems, 2nd edn. American Society of Agricultural and Biological Engineers, Ann Arbor, pp 120–159

Taylor AS, Ashcroft GL (1972) Physical Edaphology: The physics of irrigated and nonirrigated soils. WH Freeman and Company, San Francisco

Warrick AW (2002) Soil physics companion. CRC press, Boca Raton